Hardware Design and Tests of SMURF V1 Platform for Searching Survivors in Debris Cones

Masahiro Watanabe
Tough Cyberphysical AI Research Center, Tohoku University
watanabe.masahiro@rm.is.tohoku.ac.jp

Yu Ozawa
Graduate School of Information Sciences, Tohoku University
ozawa.yu@rm.is.tohoku.ac.jp

Kenichi Takahashi
Tough Cyberphysical AI Research Center, Tohoku University
takahashi.kenichi@rm.is.tohoku.ac.jp

Eri Takane
Graduate School of Engineering, Tohoku University
takane@rm.is.tohoku.ac.jp

Tetsuya Kimura
Department of System Safety, Nagaoka University of Technology
kimura@mech.nagaokaut.ac.jp

Soichiro Suzuki
International Rescue System Institute
suzuki@rescuesystem.org

Kenjiro Tadakuma
Tough Cyberphysical AI Research Center, Tohoku University
tadakuma@rm.is.tohoku.ac.jp

Giancarlo Marafioti
Department of Mathematics and Cybernetics, SINTEF Digital
giancarlo.marafioti@sintef.no

Terje Mugaas
Department of Mathematics and Cybernetics, SINTEF Digital
terje.mugaas@sintef.no

Miltiadis Koutsokeras
Institute of Communication and Computer Systems
miltos.koutsokeras@iccs.gr

Satoshi Tadokoro
Graduate School of Information Sciences, Tohoku University
tadokoro@rm.is.tohoku.ac.jp

ABSTRACT

When a large-scale disaster such as earthquake occurs, a huge number of victims will be trapped under debris in a wide area. Rescue activities in debris are technically not easy and endanger the first responders. There are several methods for improving safety and efficiency of rescue operation, but their availability is limited to a certain area or short operating time. Our project called CURSOR is developing tools to comprehensively search victims using a large number of ground-based robots entering debris transported by aerial drones. Here we show the development of the exploration robot collecting information with several sensors. The robot system was designed based on the requirements and performance was evaluated by ruggedization tests and mobility tests. No critical problem was found in the durability, and the mobility showed as the same as the ordinary wheel. To improve the mobility, we are planning to apply a proposed unique track mechanism.

Keywords

Search and Rescue (SaR), miniaturized mobile robot, wheeled robot, remotely operated Vehicle (ROV), emergency responder.

INTRODUCTION

Due to the recent global abnormal weather, natural disasters occur frequently, and human and economic loss has become a problem (Laurens M. Bouwer, 2011; Drago Bergholt et al, 2012). Strengthening disaster response capabilities and increasing social resilience are issues that humankind needs to solve. In particular, the rescue of lives in collapsed rubble when a large-scale disaster such as an earthquake occurs is often not possible with current rescue methods. It is required that search and rescue activities be enhanced by introducing advanced technologies.

In lifesaving, it is necessary to first detect the victim and identify the location within 72 hours (Sergio F. Ochoa et al, 2015) and provide the information to the first responders in real-time. Investing appropriate resources according to the situation at the site enables quick action to save many lives.

In order to search inside the debris, it is necessary to access an environment that is difficult for humans to physically access while ensuring the safety of the first responders while considering the environmental conditions at the disaster site. Although various methods are currently being developed and studied, some problems remain. Fiberscope cameras (Takumi Fujikawa et al, 2019) have a low ability to enter rubble and can only search on the top surface of the rubble pile. Snake-type robots (Fumitoshi Matsuno et al, 2019; J. Whitman et al, 2018) have a high ability to move on rough terrain, however, they are large and expensive, result in the use of ropes while operating, and they are limited to searching the local space near the entrance. The rescue dog (Kazunori Ohno et al, 2019; Alper Bozkurt et al, 2014) can be active for about 10 minutes each time and need a rest frequently. The scent of the victims may not spread to the rubble surface, and the dog may bark without finding the victims. Aerial vehicle (Balmukund Mishra et al, 2020; Hartmut Surmann et al, 2019) can capture the entire disaster site from the air, but the risk of collision with objects makes it difficult to get inside the rubble.

The CURSOR Project (ARTTIC, 2021) aims to develop a Search and Rescue (SaR) Kit, which integrates several key technologies into a platform, which contributes to finding victims efficiently in the rubble and grasping the situation (Authors to be disclosed, 2021). Small mobile robots and drones are developed to shorten the victim detection time and improving localization accuracy. The real-time information management, situational awareness, and rescue team safety are also improved.

This paper provides the development of a platform of a small ground-based mobile robot that enters the rubble and collects information by sensors. Our challenge is to develop hardware for robots that can penetrate and move deep into the rubble, disperse it over a wide area, collect information. The remainder of this paper is structured as follows: An overview of the CURSOR SaR Kit; Introducing the conceptual design of a wheeled-type Soft Miniaturized Underground Robotic Finders (SMURF) hardware design; mobility tests and ruggedization tests of the robot; Development of a novel mono-wheeled flexible track to improve mobility on higher steps.

OVERVIEW OF THE CURSOR SAR KIT

Figure 1 shows the overview of the CURSOR Search and Rescue (SaR) Kit. SMURF is small mobile robot with high mobility in rubble. A chemical sensing platform (Sniffer), visual camera, thermal camera, microphone, speaker, IMU, a communication module, etc. are installed. Since the gas sensor detects chemical substance markers from the human body using a VOC sensor array, it is made smaller and more sensitive, and the detection accuracy is improved by data processing. Several types of drones are developed to transport ground penetrating radar for making radargrams, tethered drones for 24/7 area monitoring, transporting, and unloading of SMURFs, and 3D mapping for advanced situational awareness. Secure and reliable communication system based on stationary and portable gateways are developed.

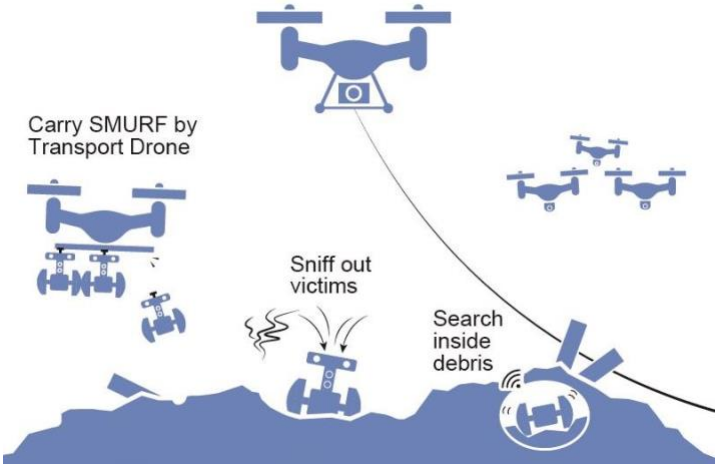

Figure 1. Overview of CURSOR SaR Kit.

REQUIREMENTS AND SPECIFICATIONS OF SMURF

The SMURF is a miniaturized robot designed and developed to use in areas where access is difficult or dangerous for humans or canine units. Some SMURFs will be deployed by hand. The others will be transported by drones and dropped at the target point. They will first penetrate the top layers of the rubble pile. Then will penetrate inside the lower layers to search for trapped victims.

Considering the purpose, SMURFs must have the ability to move across and through all variations of a collapsed structure terrain, including the maneuver through and on sand, dust, ash, mud, gravel, concrete fragments. Also, require surviving free fall and can retrieve the right position, and climb over obstacles as high as possible. The following shows the part of the technical requirements for the SMURF related to the hardware designs.

- Multiple 1 m drop resistant.
- Height of bounce less than 3%.
- IP level >=IP42.
- Max 2 hours battery life with rechargeable and replaceable battery.
- Operating temperature range -20 to +45℃ outside rubble and -15 to +65℃ inside rubble.
- Withstand 100% humidity.
- Movement on and in the debris.
- Minimize weight and size.
- Low cost and best value for the money.

DESIGN OF SMURF V1

Robot Conceptual Design

Development of SMURF consists of two stages in CURSOR. SMURF V1 is designed based on high-TRL technologies so that it works in debris cones but with limited mobility and performance as the first experimental version. SMURF V2 is planned to achieve higher capabilities by studying soft robotics and robot intelligence.

Figure 2 shows the CG model of prototype SMURF V1.0.3. It consists of the following main mechanical components; two flexible wheels, a monocoque constructed body, and a supporting tail. The tail contacts to the ground while moving forward to cancel the wheel's torque. When the wheel rotates to the opposite direction that the tail cannot support, the tail lifts and SMURF stands up so that cameras and sensors mounted on the tail would be used in a high position to the ground as possible.

Although this two-wheeled type robot may not achieve high mobility performance on rough terrains, it can construct a low-cost, compact, lightweight, and simple design, and can also easily introduce high reliable technology well-established.

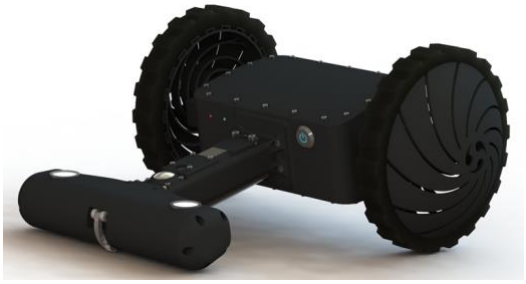

Figure 2. CG model of SMURF V1.0.3. The robot composed of two flexible active wheels and a tail.

Mechanical Design

Figure 3 shows the arrangement of the components installed in SMURF. Table 1 shows the specifications of SMURF. The prototype SMURF had dimensions of 315 mm in the width, 304 mm in the length, and 155 mm in diameter. The total mass was 910 g. Most parts were printed by a 3D printer (Markforged Mark Two, material: onyx with carbon fiber), including the main body, tail, and wheels. The components inside the body can access for maintenance by opening two large lids on the top and the bottom.

The components were carefully placed in each best/better position so that the equipped sensors can fully work its performance. A large custom main circuit board is mounted inside the body to connect all the internal electrical components. A hook is attached on the top to hang SMURF on a transport drone rail. A torsion spring stores the hook into the tail immediately after being dropped from the drone. Two high brightness LEDs are mounted on both sides of the tail end to lighten the environment in the large area. A visual camera with high sensitivity for dark conditions and a thermal camera are mounted on the tail to overlook a wider area while SMRUS is standing. A microphone and speaker are attached on the tail for two-way audio communication with the victim. IMU is mounted near the center of gravity on the main board to measure the orientation and the gravitational forces. Two 1 W motor which is approximately 10 grams is equipped to actuate the wheels. A 177 g battery is put inside the body and use as a counterweight of the tail.

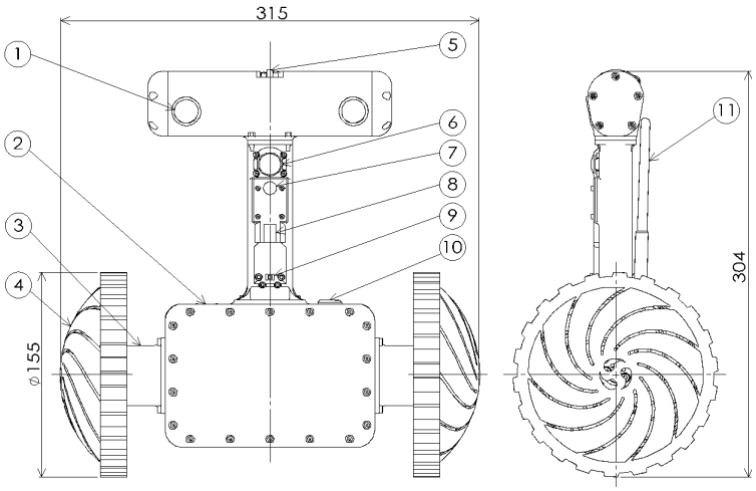

Figure 3. Components of SMURF. 1: LED. 2: Body. (i)Main board, (ii)IMU, (iii)battery is installed. 3: Geared motor. 4: Elastic wheel. 5: Hook to hang on a transport drone. 6: Visual camera. 7: Thermal camera. 8: Speaker. 9: Microphone. 10: Power switch. 11: Antenna.

Table 1. Specifications of SMURF V1.0.3

Dimensions	W315 mm H304 mm ϕ155 mm
Mass	910 g
Material	CFRP (Markforged, onyx with continuous carbon fibers)
LED (①)	3 W x 2, 180–220 lm
Main board (②−i)	Raspberry Pi Zero
IMU (②−ii)	Accel. x 3 / Gyro x 3 / Mag. x 3 / Temp.
Battery (②− iii)	7.4 V, 3300 mAh, 177 g
Geared motor (③)	1 W x 2, 33 rpm
Visual camera (⑥)	3280x2464 pixel, Viewing angle 220°.
Thermal camera (⑦)	80x60 pixel, Longwave infrared, 8 μm to 14 μm.
Speaker (⑧)	0.7 W
Microphone (⑨)	SN ratio 65 dB
Antenna (⑪)	2.4 GHz and 5 GHz

Additional sensors and components will be added in the future for more effective and efficient search missions. A chemical detection system "SNIFFER" will be installed to detect volatile chemical signatures of victims. Small VOC sensors and CO2 sensor will be developed and installed to sense some of the chemical markers. The SMURF networking will be handled by 2 Wireless Network Interface Cards (NIC) operating in Ad-Hoc Wireless Mesh Network (WMN) mode, instead of the current on-board NIC which operates in Access Point managed mode. The WMN setup allows operation without the need of an Access Point or other BSS station. The 2 NICs will operate on both the 2.4 and 5GHz RF bands respectively, allowing resilient and performant operation in different environments. Also, a localization module will be placed to detect the position of SMURF in the rubble pile using the principle of Time Difference of Arrival (TDoA) The localization module is a custom PCB based on Ultra-WideBand (UWB) technology, consisting of a SMURF included tag and multiple anchors on the perimeter of the current deployment area.

Figure 4 shows the design of the elastic wheel of SMURF. This first version was designed to be a simple circular shape that can withstand the impact dropped from a drone. It consists of a hemispherical side cover, a rubber sponge tire with grousers, and elastic spokes. Eight 2 mm thick spiral spokes, made of nylon with chopped carbon fiber, absorb radial and axial forces, and moments by its deformation. The outer chloroprene rubber sponge also absorbs shocks and makes the wheel grip to the ground. The hemisphere side cover blocks debris and other objects to get inside the spoke.

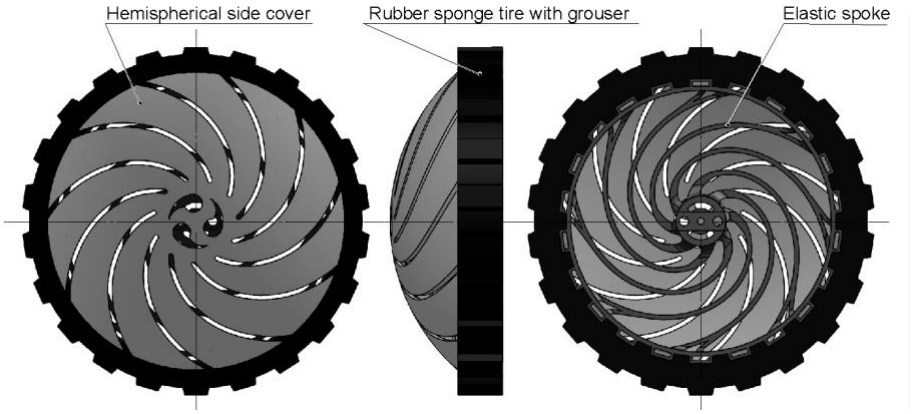

Figure 4. Design of the elastic wheel of SMURF. It absorbs radial and axial external forces, and moments by its deformation.

Electric Components and Sensors

The system diagram of electrical equipment is shown in Figure 5. Raspberry Pi zero was used as the main board due to the abundance of embedded libraries and the small size. All output module and sensor module are directly controlled by Raspberry Pi zero. Most of modules are powered by 3.3V and communicate with serial interface for extensibility. Two I2C ports are reserved for the beacon and the gas sensor. The antenna is for Wi-Fi and Bluetooth communication so that user can remotely control the robot.

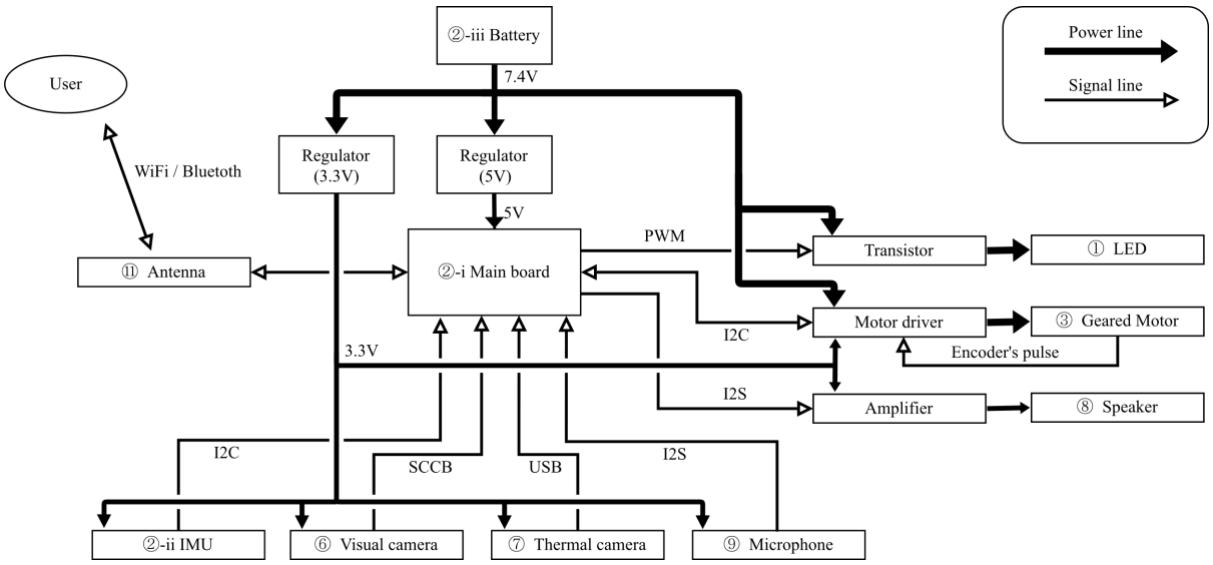

Figure 5. System diagram of electrical equipment

At the time of writing this paper, a re-designed version of the main board is being tested. The Raspberry Pi zero has been replaced by the Raspberry Pi CM 3+ and a custom motherboard has been designed and produced (Figure 6). This has been done to increase the processing power (needed for autonomy and data analysis), and to establish modular and robust connections with all the components illustrated in Figure 5.

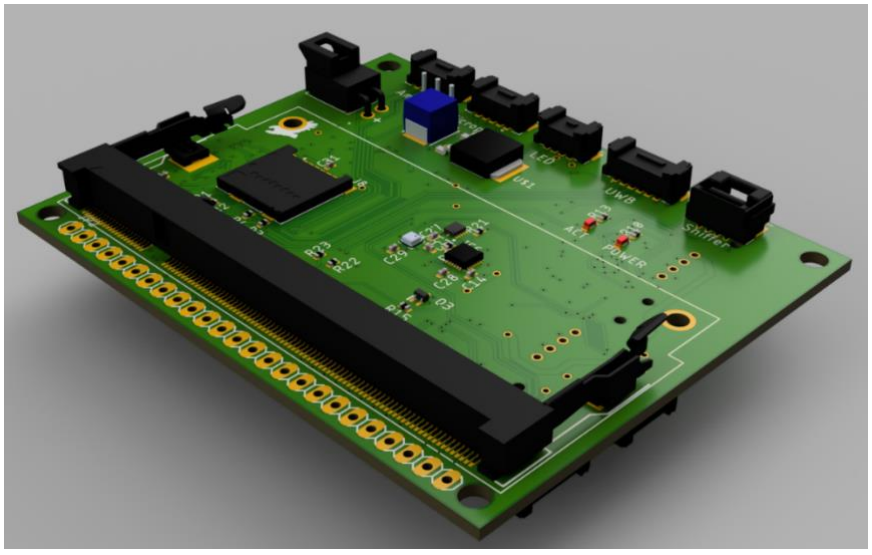

Figure 6. SMURF motherboard, dimensions: 75mm width, 61mm depth, 18.5mm height.

RUGGEDIZATION TESTS OF SMURF HARDWARE

Damages of heat, vibration, impacts, and other elements of the outer environment can cause critical problems in the SaR operation. Several tests were performed to improve the reliability of the hardware. First, ruggedization tests, including vibration, heat, humidity, drop impact, and waterproof was conducted.

All the experiments were conducted by SMURF designed which is shown in the previous section. The following

"function check" confirmed whether following equipment is working.

1. Raspberry Pi.
2. Battery checker.
3. IMU board.
4. Motor driver.
5. Speaker.
6. Microphone.
7. Visual camera.
8. Thermal camera.

The results are recorded as a log in the robot and confirmed after the test. Note that this operation check is just for confirming the presence of each operation data and does not evaluate the drift or error. The sensor is evaluated as "success" unless it is an obvious outlier.

Vibration Test

Objectives: Check the ruggedization. SMURF receives vibration during moving on rough terrains. There is a risk of causing mechanical damage such as deformation and loosening of screws, and electrical damage such as defective soldering of electronic circuits.

Test methods: The robot was fixed to the vibration table in three postures (Figure 7) using a jig. A random vibration with the power spectral density shown in Figure 8 was applied, and mechanical and electrical damage to the robot was confirmed. The test was performed in the following procedure for each fixing method following the JIS 0200: 2013 industrial standards.

1. Fixed the robot to the table while the power is turned off.
2. Vibrate the robot for 15 minutes.
3. Remove the robot from the shaking table and run the function check program.

Figure 7. Three types of fixing method on the vibration testing machine. The vibration occurs on the upward vertical direction.

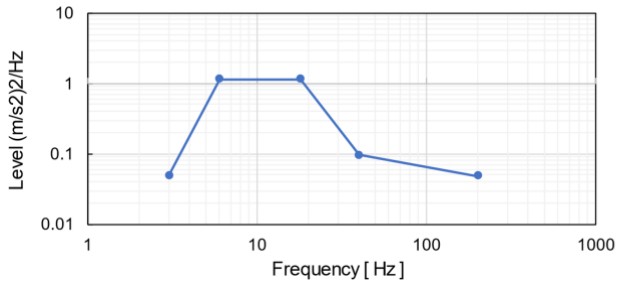

Frequency (Hz)	Level [$(m/s^2)^2$/Hz, g^2 / Hz]
3	0.048, 0.0005
6	1.15, 0.012
18	1.15, 0.012
40	0.096, 0.001
200	0.048, 0.0005

Figure 8. Condition of the random vibration (JIS 0200:2013, level3)

Results: No breakdown and fully functioning after all the tests.

Humidity Test

Objectives: Check the ruggedization. A high humidity environment may break or cause abnormal operation of electronic devices.

Test methods: The robot was placed inside a thermostatic oven (Figure 9) with a humidifying function and performed in the following procedure.

1. Place the robot in the oven while the power is turned on and raise the humidity to 96–100%.
2. Run the function check program every 1 minute. The humidity in the tank was more than 96% for 10 minutes.
3. Take the robot out from the oven and conduct function check.

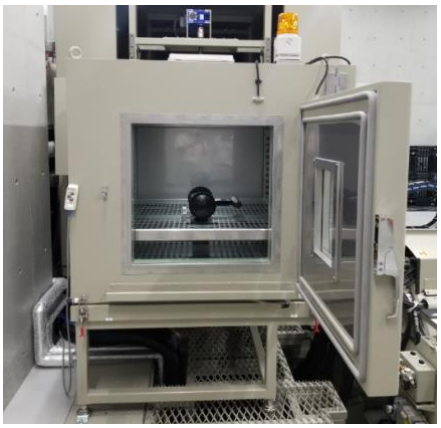

Figure 9. Thermostatic oven for humidity test

Results: After taking the robot out of the oven, the lends of the visual camera got fogged as shown in Figure 10. After leaving it at room temperature for about 15 minutes, the lends dried. Figure 11 shows the images taken with a visual camera before and immediately after the humidity test. The image taken immediately after the test shows a slight white fog in the center. In the function check, all electronic devices operated normally.

Figure 10. Fog on the lens just after humidity test

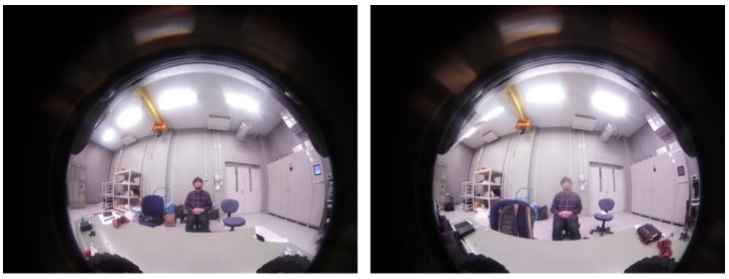

Figure 11. Pictures taken by the visual camera before and just after the humidity test

Heat Cycle Test

Objectives: Check the ruggedization of electrical equipment. SMURF is greatly affected by the outside atmosphere temperature.

Test methods: The robot was placed inside a thermostatic oven. The following is the procedure.

1. Place the robot in the oven while the power is turned off.
2. The temperature was changed for 24 hours in the range of 30 to 80℃ in a 1-hour cycle.
3. Take the robot out from the oven and conduct function check.

Results: Figure 12 shows the example of the temperature change inside the oven for three cycles. No abnormalities such as breakdowns were found in the electronic components. However, it was confirmed that the resin lid of the body was deformed by heat (Figure 13). After the test, the lid was made thicker, and ribs were added.

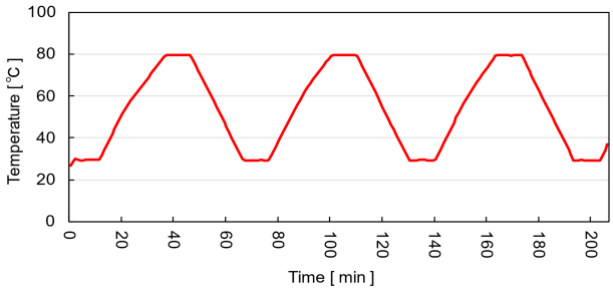

Figure 12. Measured temperature of the heat cycle test

Figure 13. Heat deformation of the lid caused by the heat cycle test

Low Temperature Test

Objectives: Check the ruggedization under freezing environment.

Test methods: The robot was placed in a thermostatic oven. The following is the procedure.

1. Place the robot in the oven while the power is turned on.
2. Freeze the oven to -18℃ for 10 minutes. Run the function check program every 1 minute.
3. Take the robot out from the oven and conduct function check.

Results: Figure 14 shows the temperature change of the oven during the test, the internal temperature of the robot, and the CPU temperature. The minimum temperature inside the robot was 3.2℃, and the minimum temperature of the CPU was 21.6℃. No abnormality was found in the function check of the robot taken out from the oven, but when the log was checked, out of the 8 function checks, communication with the motor driver failed twice. No problem was found in the maneuvering after the test.

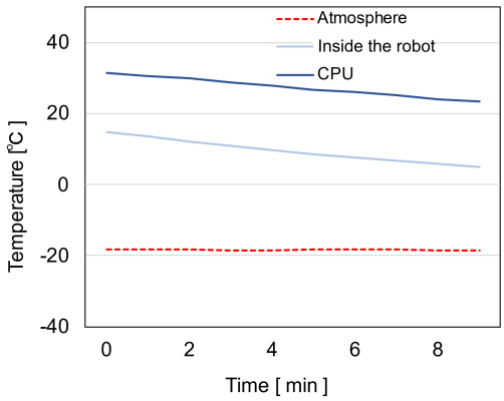

Figure 14. Measured temperatures through the low temperature test.

High Temperature Test

Objectives: Check the ruggedization under hot environment.

Test methods: The robot was placed in a thermostatic oven. The following is the procedure.

1. Place the robot in the oven while the power is turned on.
2. Raise the temperature to 30, 40, 50, 55, 60, 65 ° C every 10 minutes, and perform function test every 1 minute.
3. Take the robot out from the oven and conduct function check.

Results: Figure 15 shows the temperature change inside the oven during the test, the internal temperature of the robot, and the CPU temperature. In the relatively low-temperature range inside the oven, the CPU temperature is higher than the inside temperature due to heat generation, but there is not much difference in the high-temperature range. In this test, the lid deformed the same as the heat cycle test. No failure was found in the circuit, but the log showed the continuation of the communication failure with motor driver from the low-temperature test.

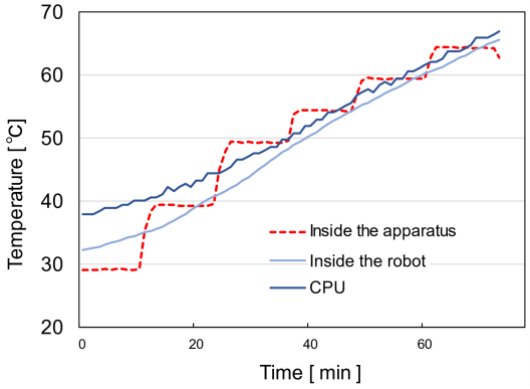

Figure 15. Temperature through the high temperature test

Waterproof Test

Objectives: Robots requires to operate in the rain. A brief waterproof test was conducted to confirm the waterproofness and water resistance of the robot.

Test methods: Two waterproof-designed parts were tested. One is the part which a gasket is inserted, and the other is part sealed with glue. As shown in Figure 16, first, the robot body was placed in the water tank, and water was dropped from above using a shower head to check for inundation. A gasket is inserted between the body and the lid. The inundation was confirmed by attaching a submersion detection sticker inside the body and checking the discoloration of the sticker after water discharge. Next, a tail was tested (Figure 17). The LEDs are glued to the tail. The following is the procedure.

1. A submersion detection sticker was attached inside the body, and the joints other than the upper and lower lids were covered with masking tape.
2. A gasket was placed, and the lid was closed with screws.

3. The body of the robot was placed horizontally on the table and installed in the water tank.
4. The shower head was tilted 60° and water was discharged to the body for 1 minute with a flow rate of 10 L/min.
5. Clear off the water droplets and open the lid. Check for discoloration of the submerged detection sticker.
6. Next, a tail was tested. The open part of the tail was closed with masking tape.
7. Water was poured from the body-connecting surface.
8. Confirmed whether water had entered from around the LED.

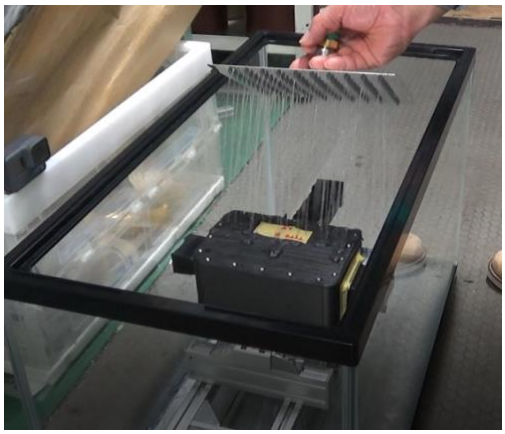

Figure 16. Waterproof test for the body

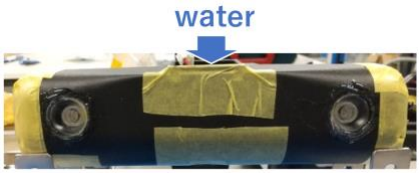

Figure 17. Waterproof test for the tail

Results: The condition inside the body after the test is shown in Figure 18. No inundation was found inside the body. Also, no water leaching was observed at the tip of the tail.

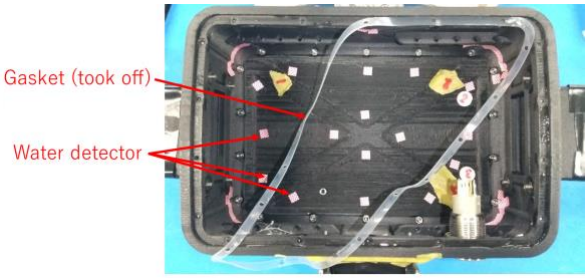

Figure 18. Result of the waterproof test for the body

PERFORMANCE TESTS OF SMURF HARDWARE

Battery duration, the visual camera, and the thermal camera were tested. In addition, experiments to measure the basic performance of climbing steps, gaps, inclined surface, and stop distance on the inclined surface was carried out.

Battery Duration Test

Objectives: Robot duration is equivalent to the battery capacity and power consumption. In order to confirm the battery consumption during standby, the transition of the battery voltage was measured.

Test methods: The power of the robot was turned on and stand the robot without using any sensors other than the current-voltage module, and measure the output current and voltage of the battery. A fully charged 2-cell 3300 mAh LiPo battery was used, and the test was performed according to the following procedure.

Results: Figure 19 shows the transition of the output current and voltage of the battery. The battery reached the recommended operating voltage limit (7.0V) in 24 hours and 50 minutes after being fully charged. After that, the voltage dropped sharply.

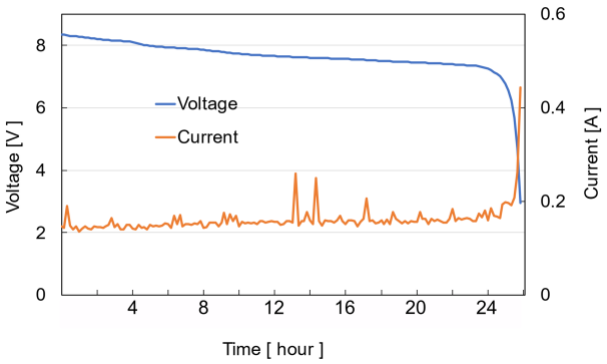

Figure 19. Voltage and current of the battery

Visual Camera and Thermal Camera Test

Objectives: Robot is required to recognize victims even in the dark by combining a visual camera with a thermal camera. We conducted a test to confirm the camera's recognition ability under different illuminance.

Test methods: We took pictures of a human sitting on a chair in front of the robot while changing the conditions of the room illumination and the robot illumination (1)-(4) in Figure 20.

Results: Figure 20 shows the values of the illuminometer and the images acquired by the two cameras under each illuminance condition. The left is the visual camera, and the right is the thermal camera. It can be seen that a visual camera is effective when the room is bright, and thermal camera is effective when the room is dark.

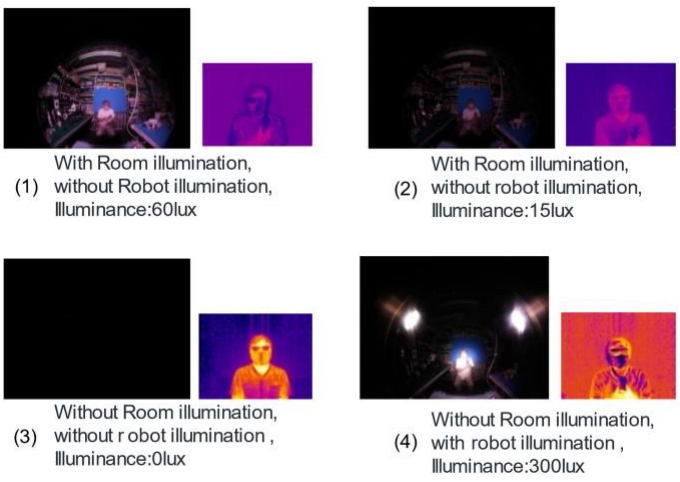

Figure 20. Pictures taken by the visual camera and the thermal camera

Hole Entering Test

Objectives: Measure the minimum size of the gap that the robot can enter.

Test methods: The robot entered the vertical and horizontal holes made of oriented strand board (OSB) shown in Figure 21, and the minimum size of the holes that the robot could pass through was measured. The following is the procedure.

1. Adjusted the size of the hole and place the robot in front of the hole.

2. Move the robot straight forward toward the hole up to 3 times.
3. If the hole can be passed within 3 trials, it is considered that the hole of that size can be passed, and one side of the hole is narrowed by 2 cm.
4. Performs procedure 1. to 3. on both sides of the hole to find the minimum value that can be passed through each.

Entering the hole was performed in two ways for the vertical hole: entering the front (entering angle 0 °) and adjusting the angle appropriately by manual control. For the side hole, only entering from the front was performed.

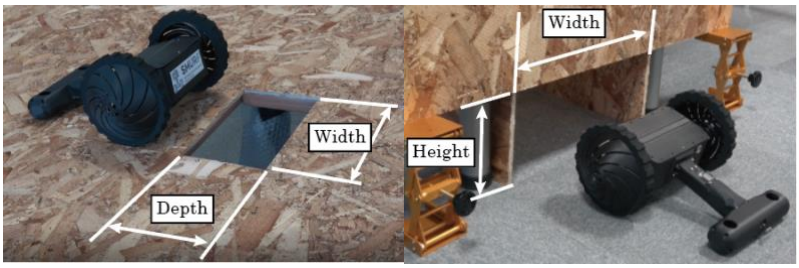

Figure 21. Setup of the vertical hole (left) and horizontal hole (right)

Results: The test results are shown in Table 2. The size of the hole that could be passed when entering from the front was almost the same as the width and height of the robot (315x155 mm). For the vertical hole whose entering angle was adjusted manually, it was possible to pass through a narrower hole by inserting the wheels one by one. Figure 22 shows procedure to pass the smallest hole (280x160mm).

Table 2. Results of the hole entering test

Entering angle	Hole direction	Minimum size of the square hole
0 deg	Vertical	320 x 160 mm (W x D)
	Horizontal	320 x 160 mm (W x D)
Manually random	Horizontal	280 x 160 mm (W x D) (Geometrically minimum)

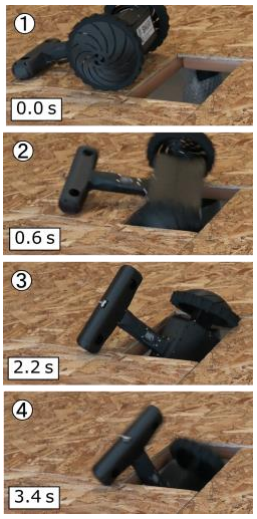

Figure 22. Entering Horizontal hole 280 x 160mm

Mobility of Gap and Hurdle

Objectives: There are obstacles of various sizes and shapes in the rubble. In order to confirm the basic ability of the robot to overcome obstacles, we conducted a mobility test to overcome three types of obstacles.

Test methods: The test was conducted according to "Standard Test Method for Evaluating Emergency Response Robot Capabilities: Mobility: Confined Area Obstacles: Hurdles" (ASTM E2802-11) and "Standard Test Method for Evaluating Emergency Response Robot Capabilities: Mobility: Confined Area Obstacles: Gap" (ASTM E2801-11) in "Standard Test Methods for Response Robots" (Adam Jacoff, 2021), made by ASTM International, which are widely used for evaluating disaster response robots and drones (The InterAgency Board, 2021; NFPA2400, 2021)

The entire test equipment is shown in Figure 23. The photo shows the arrangement of the hurdle with a pipe during the experiment. The test equipment consists of two stages made of lauan board, and by arranging the two stages apart, a groove-shaped obstacle (gap) is created, and a 5 mm thick plate is sandwiched under the stage on the far-right side of the image. By combining with the stage on the left front, an obstacle (hurdle) on the step was created. In addition, a freely rotating 38 mm diameter pipe was installed in front of the hurdle to make it a hurdle with a pipe. A side view of each obstacle is shown in Figure 24. The following is the procedure.

1. The test equipment was set, and the robot was placed on the left stage.
2. The robot was manually operated to make 10 reciprocations between the left and right stages. At this time, the robot was moved until the full body completely got inside each stage.
3. If the robot succeeds in 10 round trips without failing even once, it is judged to be a success.
4. For each obstacle, the maximum gap width or hurdle height that can be overcome in 5 mm increments was measured.

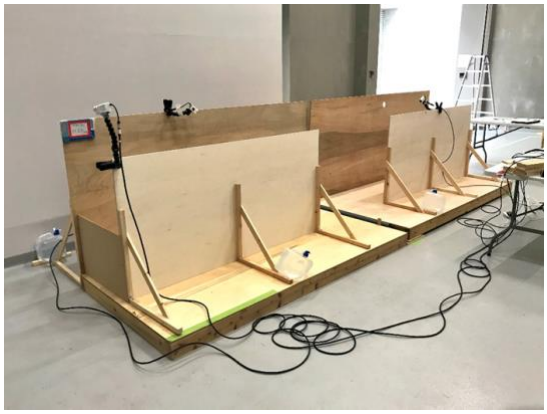

Figure 23. Test field of the maneuvering test

Figure 24. Gap, hurdle, hurdle with pipes in the test field

Results: Table 3 shows the result of each test. When overcoming a gap with a width of 135 mm, the sponge of the wheel got stuck in the gap and was unable to escape. In overcoming the hurdle, when there was a pipe, the score dropped significantly compared to when there was no pipe. It is considered difficult to overcome low-friction obstacles because it is difficult to obtain driving force only with front wheels without any rear wheels. As shown in Figure 25, it was possible to obtain some traction from the "rear wheel" by entering the hurdle at a certain angle and climb a step one wheel at a time.

Table 3. Results of the maneuvering robot

Field type	Max. Score
Gap	130
Hurdle	75
Height of the grouser (mm)	35

Figure 25. Enter the step from an oblique direction

Mobility on Inclined Planes

Objectives: Check the performance on the inclined plane.

Test methods: The test was conducted following the" Standard Test Method for Evaluating Emergency Response Robot Capabilities: Mobility: Confined Area Obstacles: Inclined Planes" (ASTM E2803-11). The test equipment was made by drawing a line with gum tape on a stage made of OSB plywood (Figure 26). The test was carried out by going back and forth in a 0.8 m square area separated by a tape. The test procedure is as follows.

1. The robot was placed at the starting point at the lower left of the plane.
2. The robot was manually operated and made 10 round trips between the start point and the end points.
3. If the robot succeeds in 10 round trips to all the end points without failing, it is judged to be success.
4. The maximum angle of the plane that can be traveled was obtained by changing the angle in 5° increments.

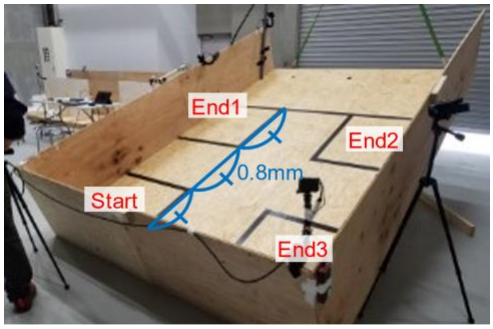

Figure 26. Setup of the inclined plane. Three types of end points was tested.

Results: The robot was able to travel vertically, horizontally and diagonally on a slope of up to 20 degrees. The result may change due to the frictional coefficient between the sponge tire and the ground material.

Drop Test

Objectives: The robot is thrown into the rubble from a height of about 1 m by a transport drone. When landing, it is desirable to stand still without being far from the drop point. In addition, it is necessary to withstand the impact of dropping. A drop test was conducted to measure the stationary distance when the robot landed on a slope and to confirm its durability against the impact of a drop.

Test methods: The robot was dropped from a distance of 1 m vertically upward from the landing point with respect to the slope used in the slope running test, and the distance on the slope (Figure 27) that moved to the final stopped position was measured. At the time of dropping, the tail of the robot was held up and the tip of the tail was held by hand. Regarding the orientation when dropping the robot, we conducted experiments in the horizontal direction and the orthogonal direction. The experiment was carried out according to the following procedure for each drop direction and inclination angle of the slope.

1. With the power turned on, the robot was dropped from a height of 1 m from the slope.
2. The distance between the landing point and the stopped point on the slope was measured.
3. Check if the robot has any mechanical trouble or not and perform the function check.
4. Repeat steps 1. to 3. 10 times.

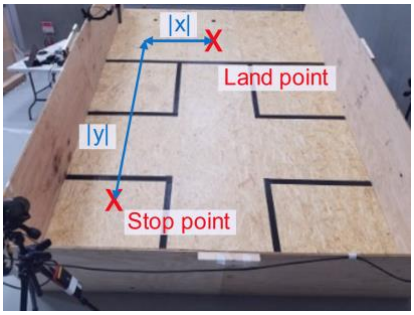

Figure 27. Setup of the drop test

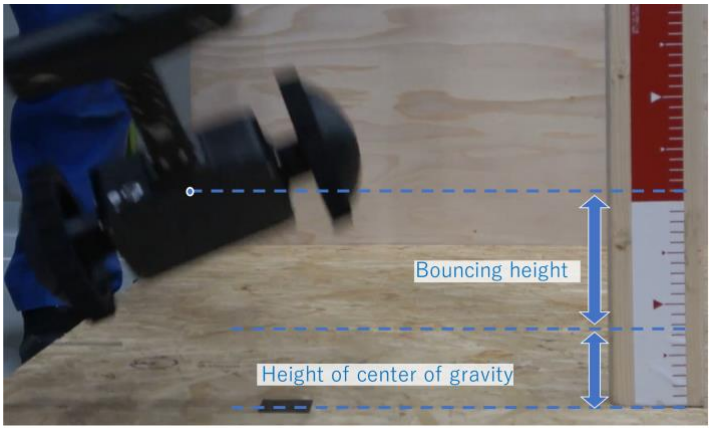

Figure 28. Bounce measuring

Results: The coefficient of restitution was measured to 0.16 by bounce measuring (Figure 28). Table 4 shows the results under each experimental condition. If the robot could not stand still on the slope and touched the wall of the test equipment, it was considered as a failure and was not included in the data. Although no mechanical or electrical damage was observed on the robot under test, it was confirmed that the push-type power switch was turned off by the impact of landing. After the test, the power switch was changed to a toggle switch.

Table 4. Specifications of the mobile robot

Direction	Inclination	| x | (Ave, SD, Max)	| y | (Ave, SD, Max)	*Failure
Parallel	10°	245, 89, 340 (mm)	646, 189, 940 (mm)	0
Parallel	15°	237, 151, 560 (mm)	1781, 370, 2350 (mm)	0
Orthogonal	10°	139, 107, 370 (mm)	603, 119, 755 (mm)	0
Orthogonal	15°	168, 139, - (mm)	1281, 314, - (mm)	2
Orthogonal	20°	53, 27, - (mm)	2315, 151, - (mm)	8

MECHANISM FOR HIGHER MOBILITY PERFORMANCE

In general, wheeled type robots cannot climb steps higher than the radius of the wheel. Thus, the mobility performance is limited when the robot size cannot be increased because of several reasons such as the robot must move inside the debris and enter a small hole. In contrast, continuous tracks with flippers generally have high mobility performances. However, its large weight is not suitable for transporting by a drone.

To overcome the problems, we developed mono-wheeled track; a novel mobile mechanism composed of an elastic belt that can adapt to irregular shape obstacles as shown in Figure 29 (Yu Ozawa et al, 2020). The proposed track could climb 145% higher steps than its diameter, which is 2.9 times higher steps than the conventional wheeled robot. Refinement of the design, such as improvement of durability, impact resistance, move on soft ground, improve step climbing performance, and optimize the track structure will take place for the next step, and ruggedization tests will be conducted for the future use in SMURF V2.

Figure 29. Mono-wheeled track capable of climbing high steps. The size is 350 mm in the length and 242 mm in the width, and 110 mm in the height. The left figure shows the overview of the track. The right figure shows the track climbing concrete blocks while adapting to the complicated terrain.

CONCLUSIONS

In this paper, the development of a two-wheel type robot for debris exploration which provides tools for search and rescue. Several tests were conducted to confirm durability and mobility of the robot. Through the vibration test, humidity test, high/low temperature tests, waterproof test, drop test, there were no critical problems such as breakdown or malfunction found. At the camera test, the robot showed enough capability to detect humans at the dark place. The battery life is confirmed to meet requirements by battery duration test. Since the robot is the prototype focusing on integration of the several sensors, its mobility has room for improvement. The capability for getting over the obstacles particularly shown in gap and hurdle tests show as the same as the ordinary wheeled robot which may not be enough for searching around in the environment with many crushed concrete blocks and broken wood. In the future, we will install our new track mechanism (SMURF V2) and conduct durability and the mobility test. Also, swarm systems with automatic control and human detection under debris will be developed and tested. Field tests will be conducted with the first responders to evaluate the usability and performance.

ACKNOWLEDGMENT

This work was done as a part of CURSOR project. The CURSOR project has received funding from the European Union's Horizon 2020 research and innovation programme under grant agreement No 832790 and from the Japan Science and Technology Agency's SICORP framework under grant No. JPMJSC1810. The opinions expressed in this document reflect only the author's view and reflects in no way the European Commission's opinions. The European Commission is not responsible for any use that may be made of the information it contains.

REFERENCES

ARTTIC. CURSOR - Accelerating Search and Rescue Operations. Retrieved February 10, 2021, from https://www.cursor-project.eu/

Authors to be disclosed (2021) Accelerating Urban Search and Rescue Operations: The CURSOR Project, *Proc. ISCRAM 2021*. (Submitted)

Bergholt, D., & Lujala, P. (2012). Climate-related natural disasters, economic growth, and armed civil conflict. *Journal of Peace Research*, *49*(1), 147–162.

Bouwer, L. M. (2011). Have Disaster Losses Increased Due to Anthropogenic Climate Change? *Bulletin of the American Meteorological Society*, *92*(1), 39–46.

Bozkurt, A., Roberts, D. L., Sherman, B. L., Brugarolas, R., Mealin, S., Majikes, J., Yang, P., Loftin, R. (2014). Toward Cyber-Enhanced Working Dogs for Search and Rescue. *IEEE Intelligent Systems*, *29*(6), 32–39.

Fujikawa, T., Yamauchi, Y., Ambe, Y., Konyo, M., Tadakuma, K., & Tadokoro, S. (2019). Development of Practical Air-floating-type Active Scope Camera and User Evaluations for Urban Search and Rescue. *2019 IEEE International Symposium on Safety, Security, and Rescue Robotics (SSRR)*, Würzburg, Germany.

Jacoff, A. Guide for Evaluating, Purchasing, and Training with Response Robots Using DHS-NIST-ASTM International Standard Test Methods. Retrieved February 10, 2021, from https://www.nist.gov/system/files/documents/el/isd/ks/DHS_NIST_ASTM_Robot_Test_Methods-2.pdf

Matsuno, F., Kamegawa, T., Qi, W., Takemori, T., Tanaka, M., Nakajima, M., Tadakuma, K., Fujita, M., Suzuki, Y., Itoyama, K., Okuno, H. G., Bando, Y., Fujiwara, T., Tadokoro, S. (2019). Development of Tough Snake Robot Systems. *Springer Tracts in Advanced Robotics Disaster Robotics*, 267–326.

Mishra, B., Garg, D., Narang, P., & Mishra, V. (2020). Drone-surveillance for search and rescue in natural disaster. *Computer Communications*, *156*, 1–10.

NFPA 2400: Standard for Small Unmanned Aircraft Systems (sUAS) Used for Public Safety Operations. Retrieved February 10, 2021, from https://www.nfpa.org/codes-and-standards/all-codes-and-standards/list-of-codes-and-standards/detail?code=2400

Ochoa, S. F., & Santos, R. (2015). Human-centric wireless sensor networks to improve information availability during urban search and rescue activities. *Information Fusion*, *22*, 71–84.

Ohno, K., Hamada, R., Hoshi, T., Nishinoma, H., Yamaguchi, S., Arnold, S., Yamazaki, K., Kikusui, T., Matsubara, S., Nagasawa, M., Kubo, T., Nakahara, E., Maruno, Y., Ikeda, K., Yamakawa, T., Tokuyama, T., Shinohara, A., Yoshinaka, R., Hendrian, D., Chubachi, K., Kobayashi, S., Nakashima, K., Naganuma, H., Wakimoto, R., Ishikawa, S., Miura, T., Tadokoro, S. (2019). Cyber-Enhanced Rescue Canine. *Disaster Robotics. Springer Tracts in Advanced Robotics*, *128*, 143–193.

Ozawa, Y., Watanabe, M., Tadakuma, K., Takane, E., Marafioti, G., & Tadokoro, S. (2020). Mono-Wheeled Flexible Track Capable of Climbing High Steps and Adapting to Rough Terrains. *2020 IEEE International Symposium on Safety, Security, and Rescue Robotics (SSRR)*, 148–153, Abu Dhabi, UAE.

Surmann, H., Worst, R., Buschmann, T., Leinweber, A., Schmitz, A., Senkowski, G., & Goddemeier, N. (2019). Integration of UAVs in Urban Search and Rescue Missions. *2019 IEEE International Symposium on Safety, Security, and Rescue Robotics (SSRR)*, 203–209, Würzburg, Germany.

The InterAgency Board. 03OE-07-ROBT. Retrieved February 10, 2021, from http://www.interagencyboard.org/

Whitman, J., Zevallos, N., Travers, M., & Choset, H. (2018). Snake Robot Urban Search After the 2017 Mexico City Earthquake. *2018 IEEE International Symposium on Safety, Security, and Rescue Robotics (SSRR)*.